

Available online at www.sciencedirect.com



Nuclear Physics B Proceedings Supplement 00 (2021) 1-5

Nuclear Physics B Proceedings Supplement

Precision predictions for direct gaugino and slepton production at the LHC

B. Fuks

CERN, PH-TH, CH-1211 Geneva 23, Switzerland;

Institut Pluridisciplinaire Hubert Curien/Département Recherches Subatomiques, Université de Strasbourg/CNRS-IN2P3, 23 Rue du Loess, F-67037 Strasbourg, France

M. Klasen, D.R. Lamprea, M. Rothering

 $Institut\ f\"ur\ Theoretische\ Physik,\ Westf\"alische\ Wilhelms-Universit\"at\ M\"unster,\ Wilhelm-Klemm-Straße\ 9,\ D-48149\ M\"unster,\ Germany\ Minster,\ Germany\ M$

Abstract

The search for electroweak superpartners has recently moved to the centre of interest at the LHC. We provide the currently most precise theoretical predictions for these particles, use them to assess the precision of parton shower simulations, and reanalyse public experimental results assuming more general decompositions of gauginos and sleptons

Keywords:

Supersymmetry, QCD, LHC

1. Introduction

For many theoretical and phenomenological reasons, supersymmetry (SUSY) remains one of the best motivated extensions of the Standard Model (SM) of particle physics. The strongly interacting superpartners in the Minimal SUSY SM (MSSM), the first- and second generation squarks and gluinos, are largely restricted after the first LHC run at 7 and 8 TeV centre-of-mass energy to be heavier than 1 TeV. However, this is not the case for stops, which play a central role in explaining the relatively large mass of the SM-like Higgs boson, and the electroweakly interacting sleptons and gauginos, which provide natural candidates for the dark matter in the universe. The search for these particles has therefore recently moved to the centre of interest at the LHC.

LHC analyses on SUSY particle searches rely heavily on precision calculations of SM backgrounds and SUSY signals. At next-to-leading order (NLO) of QCD, SUSY production cross sections have been calculated more than a decade ago [1, 2, 3, 4, 5, 6, 7]. More recently, resummation methods have been applied at next-to-leading logarithmic (NLL) accuracy [8]. Here, we

present our NLO+NLL calculations for direct gaugino [9, 10, 11, 12] and slepton [13, 14, 15, 16] production near threshold and close to vanishing transverse momentum (p_T), use them to assess the precision of parton shower simulations, and reanalyse public experimental results assuming more general decompositions of gauginos and sleptons.

2. Resummation

The hadronic cross section for the production of SUSY particles at the LHC

$$\sigma_{pp} = f_{a/p}(x_a, \mu_f) \otimes f_{b/p}(x_b, \mu_f) \otimes \sum_{n=0}^{\infty} \alpha_s^n(\mu_r) \sigma_{ab}^{(n)}(\mu_r, \mu_f)$$
(1)

is obtained by a convolution of the parton densities (PDFs) $f(x, \mu_f)$, that depend on the partonic momentum fraction x and the factorisation scale μ_f , with the partonic cross section σ_{ab} , that can be expanded in powers of the strong coupling constant $\alpha_s(\mu_r)$ running with the renormalisation scale μ_r .

Near production threshold, where the ratio of the squared invariant mass M^2 of the produced particle pair over the partonic centre-of-mass energy s, $z = M^2/s$, approaches unity, the cross section exhibits logarithim enhancements,

$$\sigma_{q\bar{q}}^{(n)}(z) = \sum_{m=0}^{2n-1} c^{(m)} \left[\frac{\ln^m (1-z)}{(1-z)} \right]_+.$$
 (2)

After applying a Mellin transform, e.g.

$$\left[\frac{\ln^m(1-z)}{(1-z)}\right] \to \ln^{m+1}(N),\tag{3}$$

these logarithmically enhanced terms, coming from soft gluon radiation, can be resummed to all orders,

$$\sigma_{q\bar{q}}^{(n)}(N) = H_{q\bar{q}} \cdot \exp\left(\tilde{c}^{(1)}\ln(N) + \tilde{c}^{(2)} + ...\right),\tag{4}$$

where H represents the hard, non-singular part and $\tilde{c}^{(i)}$ are universal coefficients. Since also the dominant collinear $1/N_C$ terms (N_C being the number of colours in QCD) are universal, they can also be exponentiated in a so-called "collinear improved" resummation calculation [17].

A second critical region is encountered when the transverse momentum of the produced particle pair tends to zero, $p_T \rightarrow 0$. There, the cross section behaves as

$$\sigma_{q\bar{q}}^{(n)}(p_T) = \sum_{m=0}^{2n-1} c^{(m)} \left[\frac{1}{p_T^2} \ln^m \left(\frac{M^2}{p_T^2} \right) \right]_+.$$
 (5)

After applying a Fourier transform,

$$\left[\frac{1}{p_T^2} \ln^m \left(\frac{M^2}{p_T^2}\right)\right]_+ \to \ln^{m+1} \left(\frac{M^2 b^2}{b_0^2} + 1\right) \tag{6}$$

with $b_0 = 2e^{-\gamma_E}$, the logarithms can again be resummed to all orders,

$$\sigma_{q\bar{q}}^{(n)}(N) = H_{q\bar{q}} \cdot \exp\left(\tilde{c}^{(1)}\ln(b) + \tilde{c}^{(2)} + \ldots\right). \tag{7}$$

Since the threshold and transverse-momentum logarithms are of the same kinematic origin, i.e. soft gluon radiation, they can also be resummed jointly in (N, b) space.

To achieve the best possible accuracy over the full kinematic ranges, the fixed-order and resummed results are added. However, since the logarithmically enhanced terms are present in both parts, this overlap must be subtracted to avoid double counting.

$$\sigma_{ab} = \sigma_{ab}^{\text{f.o.}} + \sigma_{ab}^{\text{res.}} - \sigma_{ab}^{\text{exp.}}.$$
 (8)

Table 1: Our constrained MSSM benchmark point with $\tan \beta = 10$ and $A_0 = 0$ GeV. All masses are given in units of GeV, and the gluino and average squark masses are rounded to 5 GeV accuracy.

| $(m_{1/2}, m_0)$ | $m_{\tilde{g}}$ | $\langle m_{\tilde{q}} \rangle$ | $BR(\tilde{\chi}_2^0 \to \tilde{\chi}_1^0 h)$ |
|------------------|-----------------|---------------------------------|---|
| (600, 400) | 1370 | 1275 | 92% |

Distributions in the measured quantities M and p_T are then obtained by applying an inverse Mellin transform

$$M^2 \frac{\mathrm{d}\sigma_{AB}(\tau)}{\mathrm{d}M^2} = \frac{1}{2\pi i} \int_{C_N} \mathrm{d}N \tau^{-N} M^2 \frac{\mathrm{d}\sigma_{AB}(N)}{\mathrm{d}M^2}$$
(9)

with the so-called minimal prescription, where an integration contour C_N is defined by $N = C + ze^{\pm i\phi}$ and $z \in [0, \infty[$, and an inverse Fourier transform

$$\frac{\mathrm{d}\sigma}{\mathrm{d}p_T^2} = \frac{M^2}{s} \int_0^\infty \mathrm{d}b \, \frac{b}{2} \, J_0(bp_T) \, \mathrm{d}\sigma(b) \tag{10}$$

with a deformed contour $b = (\cos \phi + i \sin \phi)t$ and $t \in [0; \infty[$ for a proper treatment of all encountered poles in the complex plane.

3. Gauginos

Using the resummation formalisms described briefly above, we demonstrate the impact of our precision predictions for gaugino pair production at the LHC with a centre-of-mass energy of \sqrt{s} = 8 TeV at the constrained MSSM benchmark point defined in Tab. 1. It features sufficiently high squark and gluino masses, that are not yet excluded, and an interestingly large branching fraction of the second lightest neutralino into the lightest neutralino and the SM-like Higgs boson. The neutralino/chargino masses are 250 GeV for $\tilde{\chi}_1^0$, 472 GeV for $\tilde{\chi}_2^0/\tilde{\chi}_1^{\pm}$ and 766 for $\tilde{\chi}_{3,4}^0/\tilde{\chi}_2^{\pm}$, and the corresponding total cross sections are shown in Tab. 2. As one can see, they are often increased, in particular from LO to NLO and, as one approaches the production threshold, also from NLO to NLL, and the scale uncertainty is always considerably stabilised.

It is interesting to compare the NLL threshold resummed results with a Monte Carlo prediction at LO using the multi-parton generator MadGraph [18] and the PYTHIA [19] parton shower. As one can see in Fig. 1, the NLL+NLO invariant mass distribution (red, thick full) agrees in general very well with the Monte Carlo results obtained after matching matrix elements containing no (green, dotted), one (blue, dashed), and up to two (red, dot-dashed) additional jets to parton showering. As the NLO+NLL calculation does not contain more

Table 2: Total cross sections (in fb) for the production of various gaugino pairs and their associated scale and PDF uncertainties for the LHC running at a center-of-mass energy of $\sqrt{s} = 8$ TeV at our benchmark point. The PDF uncertainties are not shown for the LO results.

| $\tilde{\chi}_i \tilde{\chi}_j$ | LO | NLO | NLO+NLL |
|-------------------------------------|---|--|--|
| $\tilde{\chi}_1^0 \tilde{\chi}_1^0$ | $0.13^{+8.6\%}_{-7.5\%}$ | $0.16^{+3.5\%}_{-3.4\%}{}^{+3.3\%}_{-2.3\%}$ | $0.16^{+0.2\%}_{-0.3\%}{}^{+3.5\%}_{-2.4\%}$ |
| $\tilde{\chi}_2^0 \tilde{\chi}_1^-$ | 1.63 ^{+10.0%} _{-8.6%} | $1.88^{+1.8\%}_{-2.4\%}{}^{+4.1\%}_{-3.1\%}$ | $1.86^{+0.6\%}_{-1.2\%}{}^{+4.1\%}_{-3.1\%}$ |
| $\tilde{\chi}_1^+ \tilde{\chi}_2^0$ | $4.73^{+9.8\%}_{-8.4\%}$ | $5.28^{+1.8\%}_{-2.4\%}{}^{+3.9\%}_{-2.5\%}$ | $5.22^{+0.3\%}_{-0.6\%}{}^{+4.0\%}_{-2.5\%}$ |
| $\tilde{\chi}_1^+ \tilde{\chi}_1^-$ | $3.13^{+9.8\%}_{-8.4\%}$ | $3.57^{+1.9\%}_{-2.5\%}{}^{+3.5\%}_{-2.2\%}$ | $3.52^{+0.4\%}_{-0.7\%}{}^{+3.7\%}_{-2.3\%}$ |
| $\tilde{\chi}_2^+ \tilde{\chi}_3^0$ | $0.16^{+14.2\%}_{-11.6\%}$ | $0.17^{+3.5\%}_{-4.2\%}{}^{+6.1\%}_{-3.8\%}$ | $0.17^{+1.0\%}_{-1.8\%}{}^{+6.1\%}_{-3.8\%}$ |
| $\tilde{\chi}_2^+ \tilde{\chi}_4^0$ | $0.15^{+14.3\%}_{-11.7\%}$ | $0.16^{+3.4\%}_{-4.2\%}{}^{+6.1\%}_{-3.9\%}$ | $0.16^{+1.1\%}_{-1.8\%}{}^{+6.1\%}_{-4.0\%}$ |
| $\tilde{\chi}_2^+ \tilde{\chi}_2^-$ | $0.11^{+13.6\%}_{-11.2\%}$ | $0.12^{+3.1\%}_{-3.9\%}{}^{+6.0\%}_{-3.5\%}$ | $0.12^{+1.0\%}_{-1.8\%}{}^{+6.0\%}_{-3.6\%}$ |

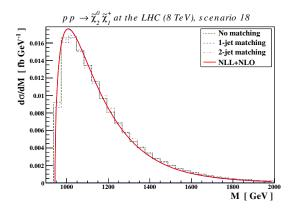


Figure 1: Distributions in the invariant mass M of a $\tilde{\chi}_2^0 \tilde{\chi}_1^+$ pair with mass 472 GeV each at the LHC with $\sqrt{s} = 8$ TeV. We compare the NLO matched to the NLL (red, thick full) distribution to the results obtained after matching matrix elements containing no (green, dotted), one (blue, dashed), and up to two (red, dot-dashed) additional jets to parton showering.

than one hard additional jet, it does, however, not allow to validate precisely the two-jet matching [20].

A comparison of NLO and NLO+NLL p_T spectra versus the corresponding MadGraph and PYTHIA predictions is shown in Fig. 2. While the NLO prediction diverges at low p_T , the NLO+NLL result shows the correct physical turnover and agrees very well with the Monte Carlo predictions. Again, the two-jet matching can not be precisely validated due to the lack of two hard jets in the NLO+NLL calculation.

4. Sleptons

The production of slepton (\tilde{l}) pairs has so far been analysed by the LHC experiments ATLAS and CMS

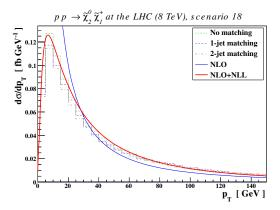


Figure 2: Distributions in the transverse momentum p_T of a $\tilde{\chi}_2^0 \tilde{\chi}_1^+$ pair with mass 472 GeV each at the LHC with $\sqrt{s}=8$ TeV. We compare fixed order at $O(\alpha_s)$ (blue, full) and NLL (red, thick full) distributions to the results obtained after matching matrix-elements containing no (green, dotted), one (blue, dashed), and up to two (red, dot-dashed) additional jets to parton showering.

using simplified models. In particular, they assume a flavour-conserving decay into a SM lepton l and the lightest SUSY particle (LSP, $\tilde{\chi}_1^0$), while all other SUSY particles, in particular the squarks and gluinos, are assumed to be heavy and to decouple. The experimental signature is then a pair of same-flavour leptons and missing transverse energy (E_T).

In our (re-)analysis [21], we take into account different slepton flavors (also $\tilde{\tau}$), both left- and right-handed sleptons (incl. mixing for staus) [22], and a different gaugino or higgsino nature of lightest neutralino [23]. The stau mass eigenstates are in particular obtained through

$$\begin{pmatrix} \tilde{\tau}_1 \\ \tilde{\tau}_2 \end{pmatrix} = \begin{pmatrix} \cos \theta_{\tilde{\tau}} & \sin \theta_{\tilde{\tau}} \\ -\sin \theta_{\tilde{\tau}} & \cos \theta_{\tilde{\tau}} \end{pmatrix} \begin{pmatrix} \tilde{\tau}_L \\ \tilde{\tau}_R \end{pmatrix}. \tag{11}$$

Their couplings to Z bosons and neutralinos are given by

$$C_Z^{(\tau)} = \left[-\frac{1}{2} + s_W^2 \right] \cos^2 \theta_{\tilde{\tau}} + \left[s_W^2 \right] \sin^2 \theta_{\tilde{\tau}}$$
(12)

$$C_N^{(\tau,L)} = \sqrt{2}e \left[s_W N_1^* + c_W N_2^* \right] \cos \theta_{\tilde{\tau}} - \left[2c_W s_W N_3^* y_\tau \right] \sin \theta_{\tilde{\tau}}$$

$$C_N^{(\tau,R)} = \left[-2\sqrt{2}e s_W N_1 \right] \sin \theta_{\tilde{\tau}} - \left[2c_W s_W N_3 y_\tau \right] \cos \theta_{\tilde{\tau}}$$

where y_{τ} denotes the tau lepton Yukawa coupling, which in the case of third-generation (s)leptons cannot be neglected. The four neutralino mixing parameters are constrained by a unitarity relation,

$$|N_1|^2 + |N_2|^2 + |N_3|^2 + |N_4|^2 = 1. (13)$$

In Fig. 3 we show total production cross sections at NLO+NLL as a function of both stau mass and mix-

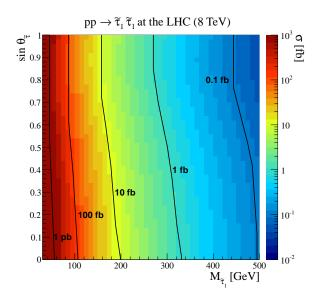


Figure 3: Total cross sections for stau pair production at the LHC, running at centre-of-mass energies of 8 TeV. We present predictions as functions of the stau mass and the stau mixing angle after matching the NLO results with threshold resummation at the NLL accuracy.

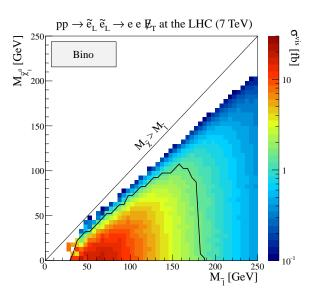
ing angle. As one can see, the cross section drops with the mass of the produced staus, but also as they become more right-handed, corresponding to larger values of $\theta_{\tilde{\tau}}$.

We have recast a recent ATLAS slepton analysis [24] to take into account the different gaugino/higgsino nature of the neutralino that results, e.g., from left-handed selectron decays. As one can see in Fig. 4, the exclusion curves for binos (top) and winos (bottom) are very similar, i.e. there is not much sensitivity to the nature of the lightest neutralino in these slepton decays.

The situation is quite different for the left-/right-handed nature of the decaying slepton, as one can see in Fig. 5. Here we assume a mixed bino-wino nature for the lightest neutralino and study the production of left-(top) and right-handed (bottom) smuons. The exclusion curves are in this case quite different, reflecting the fact that right-handed (s)leptons have weaker couplings and smaller cross sections.

5. Conclusion

The most precise electroweak SUSY particle production cross sections at NLO+NLL are by now routinely taken into account by the LHC experiments ATLAS and CMS for gaugino/higgsino and slepton searches, in particular when deriving exclusion limits. The corresponding computer code RESUMMINO has been made public and is available for use in experimental analyses and



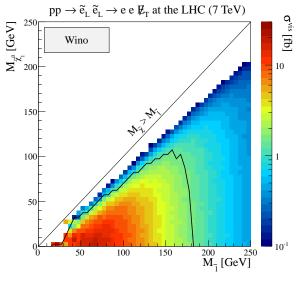
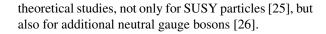
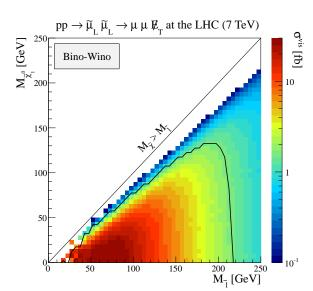


Figure 4: 95% confidence exclusion limit for left-handed selectron pair production, given in the $(M_{\tilde{l}}, M_{\tilde{\chi}_1^0})$ mass plane of a simplified model for different choices of the neutralino nature taken as bino (top) and wino (bottom). We present the visible cross section after applying the ATLAS selection strategy. The limits are extracted for 4.7 fb⁻¹ of LHC collisions at a centre-of-mass energy of 7 TeV.





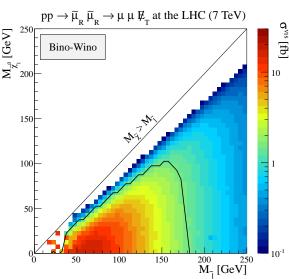


Figure 5: 95% confidence exclusion limit for left-handed (top) and right-handed (bottom) smuon pair production, given in the $(M_{\tilde{l}}, M_{\tilde{\chi}_1^0})$ mass plane of a simplified model for mixed bino-wino neutralino nature. We present the visible cross section after applying the ATLAS selection strategy. The limits are extracted for 4.7 fb⁻¹ of LHC collisions at a centre-of-mass energy of 7 TeV.

References

- W. Beenakker, R. Hopker, M. Spira and P. M. Zerwas, Nucl. Phys. B 492 (1997) 51 [hep-ph/9610490].
- [2] W. Beenakker, M. Kramer, T. Plehn, M. Spira and P. M. Zerwas, Nucl. Phys. B 515 (1998) 3 [hep-ph/9710451].
- [3] E. L. Berger, M. Klasen and T. M. P. Tait, Phys. Rev. D 59 (1999) 074024 [hep-ph/9807230].
- [4] W. Beenakker, M. Klasen, M. Krämer, T. Plehn, M. Spira and P. M. Zerwas, Phys. Rev. Lett. 83 (1999) 3780 [Erratum-ibid. 100 (2008) 029901] [hep-ph/9906298].
- [5] E. L. Berger, M. Klasen and T. M. P. Tait, Phys. Lett. B 459 (1999) 165 [hep-ph/9902350].
- [6] E. L. Berger, M. Klasen and T. M. P. Tait, Phys. Rev. D 62 (2000) 095014 [hep-ph/0005196] and Phys. Rev. D 67 (2003) 099901 [hep-ph/0212306].
- [7] M. Spira, hep-ph/0211145.
- [8] M. Kramer, A. Kulesza, R. van der Leeuw, M. Mangano, S. Padhi, T. Plehn and X. Portell, arXiv:1206.2892 [hep-ph] and references therein.
- [9] J. Debove, B. Fuks and M. Klasen, Phys. Lett. B 688 (2010) 208 [arXiv:0907.1105 [hep-ph]].
- [10] J. Debove, B. Fuks and M. Klasen, Nucl. Phys. B 842 (2011) 51 [arXiv:1005.2909 [hep-ph]].
- [11] J. Debove, B. Fuks and M. Klasen, Nucl. Phys. B 849 (2011) 64 [arXiv:1102.4422 [hep-ph]].
- [12] B. Fuks, M. Klasen, D. R. Lamprea and M. Rothering, JHEP 1210 (2012) 081 [arXiv:1207.2159 [hep-ph]].
- [13] G. Bozzi, B. Fuks and M. Klasen, Phys. Rev. D 74 (2006) 015001 [hep-ph/0603074].
- [14] G. Bozzi, B. Fuks and M. Klasen, Nucl. Phys. B 777 (2007) 157 [hep-ph/0701202].
- [15] G. Bozzi, B. Fuks and M. Klasen, Nucl. Phys. B 794 (2008) 46 [arXiv:0709.3057 [hep-ph]].
- [16] B. Fuks, M. Klasen, D. R. Lamprea and M. Rothering, JHEP 1401 (2014) 168 [arXiv:1310.2621, arXiv:1310.2621 [hep-ph]].
- [17] M. Kramer, E. Laenen and M. Spira, Nucl. Phys. B 511 (1998) 523 [hep-ph/9611272].
- [18] J. Alwall, M. Herquet, F. Maltoni, O. Mattelaer and T. Stelzer, JHEP 1106 (2011) 128 [arXiv:1106.0522 [hep-ph]].
- [19] T. Sjostrand, S. Mrenna and P. Z. Skands, JHEP **0605** (2006) 026 [hep-ph/0603175].
- [20] M. L. Mangano, M. Moretti, F. Piccinini, R. Pittau and A. D. Polosa, JHEP 0307 (2003) 001 [hep-ph/0206293].
- [21] E. Conte, B. Fuks and G. Serret, Comput. Phys. Commun. 184 (2013) 222 [arXiv:1206.1599 [hep-ph]].
- [22] G. Bozzi, B. Fuks and M. Klasen, Phys. Lett. B 609 (2005) 339 [hep-ph/0411318].
- [23] J. Debove, B. Fuks and M. Klasen, Phys. Rev. D 78 (2008) 074020 [arXiv:0804.0423 [hep-ph]].
- [24] G. Aad *et al.* [ATLAS Collaboration], Phys. Lett. B **718** (2013) 879 [arXiv:1208.2884 [hep-ex]].
- [25] B. Fuks, M. Klasen, D. R. Lamprea and M. Rothering, Eur. Phys. J. C 73 (2013) 2480 [arXiv:1304.0790 [hep-ph]].
- [26] B. Fuks, M. Klasen, F. Ledroit, Q. Li and J. Morel, Nucl. Phys. B 797 (2008) 322 [arXiv:0711.0749 [hep-ph]].